Understanding the association between climate variability and the Nile's water level fluctuations and total water storage changes during 1992-2016

M. Khaki[a,1], J. Awange[a], E. Forootan[b], M. Kuhn[a]

[a]*School of Earth and Planetary Sciences, Discipline of Spatial Sciences, Curtin University, Perth, Australia.*

[b]*School of Earth and Ocean Sciences, Cardiff University, Cardiff, UK.*

Abstract

With the construction of the largest dam in Africa, the Grand Ethiopian Renaissance Dam (GERD) along the Blue Nile, the Nile is back in the news. This, combined with Bujagali dam on the White Nile are expected to bring ramification to the downstream countries. A comprehensive analysis of the Nile's waters (surface, soil moisture and groundwater) is, therefore, essential to inform its management. Owing to its shear size, however, obtaining in-situ data from "boots on the ground" is practically impossible, paving way to the use of satellite remotely sensed and models' products. The present study employs multi-mission satellites and surface models' products to provide, for the first time, a comprehensive analysis of the changes in Nile's stored waters' compartments; surface, soil moisture and groundwater, and their association to climate variability (El Niño Southern Oscillation (ENSO) and Indian Ocean Dipole (IOD)) over the period 1992-2016. In this regard, remotely sensed altimetry data from TOPEX/Poseidon (T/P), Jason-1, and Jason-2 satellites along with the Gravity Recovery And Climate Experiment (GRACE) mission, and the Tropical Rainfall Measuring Mission Project (TRMM) rainfall products are applied to analyze the compartmental changes over the Nile River Basin (NRB). This is achieved through the creation of 62 virtual gauge stations distributed throughout the Nile River that generate water levels, which are eventually used to derive surface water storage changes. Using GRACE's total water storage (TWS), soil moisture derived from multi-models using the Triple Collocation Analysis (TCA) method, and the estimated surface water storage, Nile basin's groundwater variations are estimated. This is followed by an investigation of the impacts of climate variabilities on the compartmental changes using TRMM precipitation and large-scale ocean-atmosphere ENSO and IOD products. The results indicate a larger correlation (that are statistically significant at 95% confidence level) between the river level variations

Email address: Mehdi.Khaki@postgrad.curtin.edu.au (M. Khaki)

and precipitation changes in the central part of the basin (0.77 on average) in comparison to the northern (0.64 on average) and southern parts (0.72 on average). Larger water storages and rainfall variations are observed in the Upper Nile in contrast to the Lower Nile. A Negative groundwater trend is also found over the Lower Nile, which could be attributed to a significantly less amount of rainfall in the last decade and extensive irrigation over the region.

Keywords: Climate variability, Satellite altimetry, River Nile, Groundwater, Water level, GRACE .

1. Introduction

River Nile, arguably the longest river in the world (6800 km), has a major impact on the livelihood of over 300 million people of 11 countries within the region. This population is expected to double in the next twenty-five years (Nunzio, 2013) thereby putting extreme pressure on its water resources. Already, this pressure is building up with the upper stream countries damming the Nile to exploit on its resources. On the white Nile, already Uganda has constructed the Bujagali dam while along the Blue Nile, Ethiopia is constructing the continent's largest dam; the Grand Ethiopian Renaissance Dam (GERD) that is expected to take several years to fill. These human-induced impacts on the Nile, coupled with those of climate variability is expected to exacerbate tension with the low stream countries fearing the cut in the Nile's total volume. Its fresh water in the region that covers approximately 10% of the entire African continent is expected to continue sustaining the livelihood of the growing population thus making a large part of the African continent extremely vulnerable in aspects such as water supplies, agriculture, and industry (Woodward et al., 2007; Awulachew et al., 2012; Multsch et al., 2017). An understanding of changes in its stored water (surface, soil moisture and groundwater) and their association to climate variability/change, therefore, is crucial for environmental assessments and provides information useful for water resources management and climate impact studies. Owing to its size however, the Nile predisposes itself to remotely sensed approaches with the vast spatial and temporal coverage as opposed to ground based in-situ data collection.

Remote sensing has provided useful observations for studying water resources around the world, especially over the areas with insufficient in situ measurements (e.g., (Alsdorf et al., 2007; Zakharova et al., 2006; Papa et al., 2010)). Over the Nile River Basin, Muala et al. (2014) esti-

mated reservoir discharges of Lake Nasser and Roseires Reservoir while flood monitoring using altimetry data was carried out by Birkett et al. (1999) over Lake Victoria. Ayana et al. (2008) reviewed the application of satellite radar altimetry data in the water resource management in Ethiopia, while Uebbing et al. (2015) introduced a post-processing approach to improve the accuracy of radar altimetry measurements over African lakes such as Lake Naivasha and Lake Victoria (see also Awange et al., 2013a; Aboulela, 2012). A number of hydroclimate variability studies over the basin using various satellite remotely sensed products have been documented, e.g., the Gravity Recovery and Climate Experiment (GRACE) for studying the Nile basin's total water storage changes (e.g., Awange et al., 2008, 2014a; Hassan and Jin, 2014), satellite precipitation data for studying the basin's rainfall (e.g., Kizza et al., 2009; Awange et al., 2013b), and a combination of both ground-based and remotely sensed observations for studying the lake's water balance (e.g., Yin and Nicholson, 1998; Swenson et al., 2009).

Despite the efforts above, a comprehensive long-term study of climate variability and its association with various water storages (TWS, groundwater, surface water storage, and soil moisture) separately, as well as water level fluctuations over the entire Nile River Basin is missing. For example, although Awange et al. (2014b) studied water storage changes within the Niles main sub-basins and the related impacts of climate variability by employing Independent Component Analysis (ICA) to extract statistically independent TWS patterns over the sub-basins from GRACE and the Global Land Data Assimilation System (GLDAS) for the period 2002-2011, they did not consider the independent compartments (surface, soil moisture and groundwater) separately. Rather, they treated them as a combined entity and did not treat the fluctuations of the water level over the Nile River Basin. Fluctuations of surface water levels, which can be derived from satellite radar altimetry, are important as they can be related to seasonal variations of precipitation, evaporation, and anthropogenic use (Goita et al., 2012). Surface water storages and their variations are also important to study the interactions between land and the atmosphere and oceans (Papa et al., 2015).

The present study seeks to address these missing gaps by exploiting multi-satellites and surface models' products to study changes in the various Nile basin's water compartments (surface, soil moisture, and groundwater) and relate them to climate variability. Specifically, the study aims at (i) analyzing the long-term (1992-2016) water level fluctuations through 62 virtual altimetry-derived tide gauges along the Nile River, (ii) deriving surface water storage

from level variations in (i) above, (iii) studying compartmental water storage changes separately; surface, soil moisture, and groundwater and their association with El Niño Southern Oscillation (ENSO) and Indian Ocean Dipole (IOD) climate variability.

To provide the 62 virtual stations over the entire Nile River, TOPEX/Poseidon (T/P), Jason-1 and -2 satellite altimetry products are applied to the Nile Basin divided into Lower Nile, Central Nile, and Upper Nile (see Figure 1). The obtained water level fluctuations from these 62 virtual stations are improved using the Extremum Retracking (ExtR) algorithm (Khaki et al., 2014) and used to generate time series that are employed to derive surface water storage following the approach of Frappart et al. (2008). Furthermore, multiple models are used to estimate soil moisture variations using the Triple Collocation Analysis (TCA; Gruber et al. (2017)) over the basin, which together with TWS changes from GRACE are used to estimate Nile Basin's groundwater storage. The impact of precipitation from the Tropical Rainfall Measuring Mission Project (TRMM) on surface water variations and water storage components are thereafter explored. Previous studies (e.g., Omondi et al., 2012, 2013; Awange et al., 2014a,b; Zaroug et al., 2014; Siam et al., 2015; Conway, 2017) reported strong connections between East Africa's precipitation, water storage variations and climate variability (ENSO and IOD) phenomena.

The reminder of this study is organized as follow; the study area, datasets, and methods are presented in Sections 2 and 3, respectively. The results are discussed in Section 4 and the study is concluded in Section 5.

2. The study area and data

2.1. The Nile River Basin

The Nile's climatic conditions vary over different parts and include different climate zones (e.g., Mediterranean climate), with an average temperature of about 30°C in summers and ranging between 5°C - 10°C during winters (FAO, 1997). The arid region starts from Sudan and extends north to Egypt with average precipitation rates of 50 mm and 20 mm per year, respectively, representing almost rainless conditions during a given year (FAO, 1997; Agrawal et al., 2003). In contrast, the southern parts of the basin from the equatorial region of south-western Sudan to most of the Lake Victoria basin and the Ethiopian Highlands experience

heavy rainfall of about 1520 mm per year (Camberlin, 2009; Awange et al., 2016). A modest increase in rainfall and stored water over Lake Victoria from 2007 to 2013 after the 2002-2006 decline (Awange et al., 2008) is captured by Awange et al. (2013b) while water loss in the north-eastern lowland of Ethiopia between 2003 and 2011, in contrast to the western parts, has been observed by Awange et al. (2014a,b). Becker et al. (2010) studied the 2003-2008 water level changes in major lakes of East Africa and concluded that for lakes Victoria and Turkana basins, changes were mainly due to individual lake's storages.

The difference between climatic conditions and water availability along the Nile has become increasingly important especially for the northern areas facing increased water scarcity, i.e., Sudan and Egypt (see, e.g., Conway, 2002; Elshamy et al., 2009; Taye et al., 2011). A number of studies have investigated the interactions between different areas along the Nile River Basin and various issues, e.g., sediments (Ahmed et al., 2008) and residents income inequality (Ahmed et al., 2014). To better study the entire Nile River Basin's behaviour in regard to fluctuations and the impacts of climate, the present study divides the entire Nile Basin Basin (NRB), hereafter referred to simply as NRB, into three different regions; the Upper Nile, Central Nile, and Lower Nile (Fig. 1) approximated according to the provenance of the water as suggested in Ahmed et al. (2004).

2.2. Satellite radar altimetry

Satellite radar altimetry is an effective tool for monitoring surface water level fluctuations and has been employed for a wider range of applications (e.g., Sandwell, 1990; Fu et al., 1994; Lee et al., 2009; Hwang et al., 2010; Becker et al., 2010; Khaki et al., 2015). Altimetry, which originally was designed to monitor sea level changes, is nowadays also used for inland water lakes (see, e.g., Birkett, 1995) and rivers (e.g., Birkett et al., 2002; Berry et al., 2005; Yang et al., 2012; Tseng et al., 2013). The growing interest is largely because of its consistency and vast coverage contrary to ground-based measurements (Calmant et al., 2008). In this study, we use TOPEX/Poseidon (T/P), Jason-1, and Jason-2 data of the Sensor Geographic Data Records (SGDR), which contains 20-Hz waveform data. This includes 360 cycles of T/P covering 1992–2002, 260 cycles of Jason-1 from 2002 to 2008, and 277 cycles of Jason-2 covering 2008 to 2016. The temporal resolution of these observations is ∼9.915 days and their ground cross-track resolution is ∼280 km (Benada, 1997). T/P and Jason-1 data are both derived from the Physical Oceanography Distributed Active Archive Center (PO.DAAC) and Jason-2 data

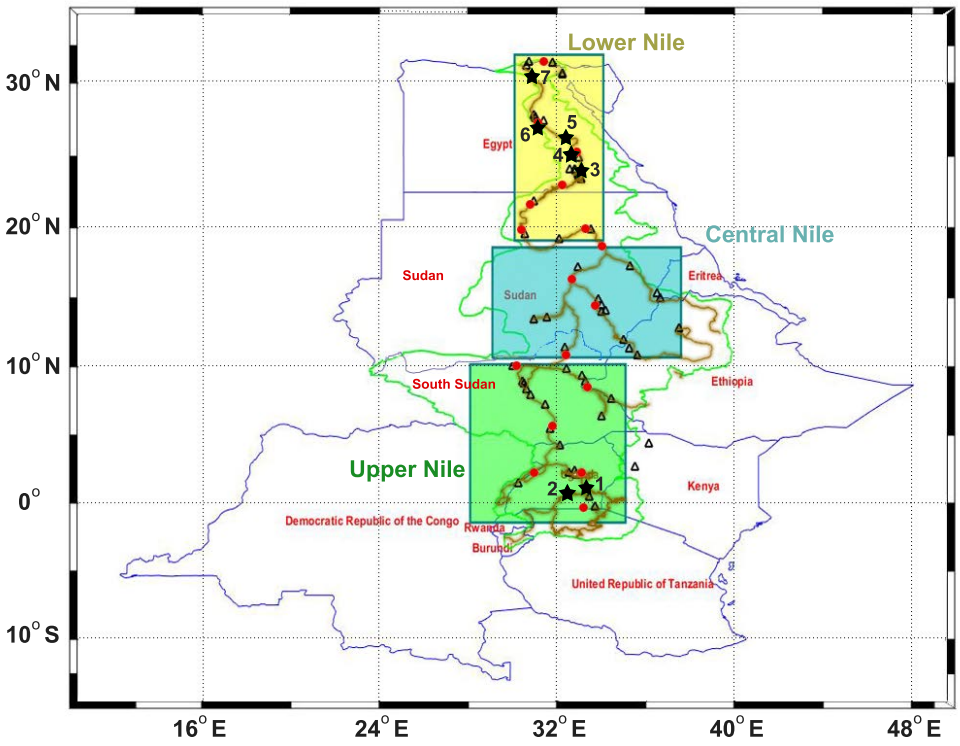

Figure 1: Location of the 62 virtual altimetry stations (black triangles) and the three study regions (Green-Upper Nile (Kenya, Uganda, Tanzania, Rwanda, Burundi, Ethiopia and South Sudan); Blue-Central Nile (Sudan, Ethiopia and Eritirea); and Yellow-Lower Nile (Egypt)) in the Nile Basin. The black stars show the positions of the gauge stations for measuring water levels while the red circles represent the locations of Hydroweb (Cretaux et al., 2011) virtual stations.

is provided by AVISO (see, e.g., Table 1). Here, we apply geophysical corrections, including solid earth tide, pole tide, and dry tropospheric (Birkett, 1995). Importantly, the waveform retracking, which refers to the re-analysis of the waveforms, a time-series of returned power in the satellite antenna (Davis et al., 1995; Gomez-Enri et al., 2009), is required to improve the accuracy of measured ranges (Brown, 1977). Here, in order to retrack satellite radar altimetry data, a developed Extrema Retracking (ExtR) algorithm proposed by Khaki et al. (2014) is applied. Our motivation to select the ExtR is due to its processing speed and its promising results over the Caspian Sea when compared to the Off Center of Gravity (OCOG, Wingham et al., 1986), the NASA β-Parameter Retracking (Martin et al., 1983), and Threshold Retracking (Davis, 1997).

The datasets are then used to build virtual time series for 62 different points (see black triangles in Fig. 1) located on the satellite ground tracks and distributed throughout the NRB.

At each virtual point, several points belonging to the same satellite cycle are considered and the median value of the retracked altimetry-based water level is computed in order to address the hooking effects (Frappart et al., 2006). This effect is derived from off-nadir measurements when a satellite locks over a water body before or after passing above it (Seyler et al., 2008; Boergens et al., 2016). Afterward, the water level variations time series derived from T/P, Jason-1, and Jason-2 (covering the period from 1992 to 2016) are merged and the combined time series converted into a monthly scale. Details of altimetry data sources and pass numbers used in this study are presented in Table 1.

2.3. GRACE

Monthly GRACE level 2 (L2) potential coefficients products up to degree and order (d/o) 90 from the ITSG-Grace2014 gravity field model (Mayer-Gürr et al., 2014) are obtained and used to generate the NRB's total water storage (TWS). Following Swenson et al. (2008), degree 1 coefficients (http://grace.jpl.nasa.gov/data/get-data/geocenter/) are replaced to account for the movement of the Earth's centre of mass. Degree 2 and order 0 (C_{20}) coefficients (http://grace.jpl.nasa.gov/data/get-data/oblateness/) are not well determined and are replaced by those from Cheng and Tapley (2004). Colored/correlated noise and leakage errors are reduced using the Kernel Fourier Integration (KeFIn) filter (Khaki et al., 2018) in a two-step post-processing scheme. The first step accounts for the measurement noise and the aliasing of unmodelled high-frequency mass variations, and the second step reduces the leakage errors.

2.4. Land hydrological models

Soil moisture data is provided from three sources; the Famine Early Warning Systems Network (FEWS NET) Land Data Assimilation System, (FLDAS-NOAH McNally et al., 2017), the WaterGAP Global Hydrology Model (WGHM; see more details in Döll et al., 2003), and ERA-Interim (Dee et al., 2011). Soil moisture outputs from these models are acquired on a monthly scale and rescaled into $1^\circ \times 1^\circ$ spatial grid and merged into a single soil moisture estimate (see Section 3.2.2) to study the soil moisture variations within the NRB as well as extracting groundwater from GRACE's TWS and surface water storage estimates (see Section 3.2).

2.5. Precipitation

Tropical Rainfall Measuring Mission Project (TRMM-3B43; version 7) products (TRMM, 2011) covering the period 1998 to 2016 are used. The data is available on a 0.25° degree resolution, which is averaged to generate 1°×1° grids before being extended to 1992 (same starting period as the altimetry data) using the Global Precipitation Climatology Center (GPCC) reanalysis version 7.0 (Schneider et al., 2015). Rainfall variations from both TRMM and GPCC datasets are used after being rescaled to the same spatial resolution as the altimetry time series.

2.5.1. ENSO and IOD

Two major climate variability indices associated with the dominant SST variability; El Niño Southern Oscillation (ENSO; Barnston et al., 1987) and Indian Ocean Dipole (IOD; Rao et al., 2002) are used to assess the association of climate variability and NRB's stored water changes. ENSO, provided by the NOAA National Centers for Environmental Information (NCEI) between 1992 and 2016, is the largest inter-annual climate variability phenomenon in the Tropical Pacific, which affects the climate of many regions of the Earth (Trenberth et al., 1990; Forootan et al., 2016). El Niño refers to the positive phase of ENSO that brings warm water towards the east of the Americas causing a climate shift over the Pacific. The opposite phase La Niña causes less than normal precipitation variability (Nazemosadat et al., 2000) in the western Pacific, and to the north of Australia. An ocean-atmosphere phenomenon measure that indicates changes in sea surface temperature in the Indian Ocean is IOD (Indian Ocean Dipole). Its data is acquired from NASA's Global Change Master Directory (GCMD). A positive IOD (often associated with El Niño) causes cooler waters (and droughts) near Australia and Southeast Asia and brings warmer than normal water and heavy rains in East Africa and India. This is broadly during a negative IOD phase (linked to La Niña). These indices are the result of interactions between the oceans and atmosphere on each corresponding area and their impact can be seen directly on rainfall that occurs around the world (Nurutami et al., 2016). Here, the interest is to understand their influences on the Nile River fluctuations, thereby, further indicating the impact of climate variability. A summary of the datasets used in the present study are presented in Table 1.

Table 1: A summary of the datasets used in this study.

Description	Source	Data resolution		Detail	Data access
		Spatial	Temporal		
Altimetry-derived level height	T/P, Jason-1	∼280 km	∼9.915	Pass numbers 18, 31, 44, 57, 83, 94, 107, 120, 133, 159, 170, 196, 209, 222, 235	http://podaac.jpl.nasa.gov
	Jason-2	∼280 km	∼9.915	Pass numbers similar to T/P, Jason-1	http://avisoftp.cnes.fr/
Precipitation	GPCC	1°	Monthly	Global precipitation climatology center (GPCC) reanalysis version 7.0	https://www.esrl.noaa.gov/psd/data/gridded/data.gpcc.html#detail
	TRMM-3B43	0.25°	Monthly	Tropical Rainfall Measuring Mission Project (TRMM) version 7.0	https://disc.gsfc.nasa.gov/datacollection/TRMM_3B43_7.html
Terrestrial water storage (TWS)	GRACE	∼300 km	Monthly		https://www.tugraz.at/institute/ifg/downloads/gravity-field-models/itsg-grace2014/
Soil moisture	WGHM	0.5°	Monthly		https://www.uni-frankfurt.de/45218093/Global_Water_Modeling
Soil moisture	ERA-Interim	0.5°	Monthly		https://www.ecmwf.int/en/forecasts/datasets/reanalysis-datasets/era-interim
Soil moisture	FLDAS	0.5°	Monthly	Famine Early Warning Systems Network (FEWS NET) Land Data Assimilation System (first soil moisture layer)	https://disc.sci.gsfc.nasa.gov/uui/datasets/FLDAS_VIC025_C_SA_M_V001/summary?keywords=FLDAS
ENSO		∼280 km	Monthly		https://www.ncdc.noaa.gov/teleconnections/enso/
IOD		∼280 km	Monthly		http://gcmd.nasa.gov/records/GCMD_Indian_Ocean_Dipole.html
Water level measurements		–	–	Ministry of Energy & Mineral Development Kampala, Uganda	http://www.energyandminerals.go.ug/

3. Method

3.1. Extrema Retracking (ExtR) and the validation of its output

In order to retrack satellite radar altimetry data over the NRB, the Extrema Retracking (ExtR) post-processing technique of Khaki et al. (2014) is employed. It is applied to the altimetry-derived waveforms to retrack datasets, what is vital for inland applications of satellite radar altimetry. The algorithm operates in three steps; (1) a moving average filter is applied to reduce the random noise of the waveforms, (2) extremum points of the filtered waveforms are identified, and (3), the leading edges among all detected extremum points are explored. Range corrections are applied using the offsets between the positions of the leading edges and their on-board values. To assess the performance of the ExtR filter, its results are evaluated against those of in-situ (see Figure 1) height variations. To this end, use is made of (i) monthly water level measurements from two gauge stations (Jinja 1992-1995 and Entebbe 1992-2009) obtained from the Ministry of Energy & Mineral Development (Kampala, Uganda), (ii) in-situ data obtained from Ismail and Samuel (2011). These are; old Aswan 1996-2009, Esna

Barrage 1996-2009, Naga Hammadi Barrage 1996-2007, and Assiut Barrage 1996-2009, and (iii), Nubaria (1997-2007) in-situ data obtained from Samuel (2014). The Root-Mean-Squared Errors (RMSE) and the correlation between the variations of altimetry-derived height time series (with and without the application of the ExtR) at the closest virtual stations to the gauge locations and in-situ time series measurements are presented in Table 2.

The Results indicate that applying retracking method increases the correlations between altimetry results and the gauge levels (0.33 on average) and improves the RMSE by 37.56% (on average). Due to a limited number of validating gauge stations in the area, water level time series from the Hydroweb project by LEGOS (Laboratoire d'Etude en Geophysique et Oceanographie Spatiale; Cretaux et al., 2011) and DAHITI (Database for Hydrological Time Series of Inland Waters; Schwatke et al., 2015) were further used. Figure 2 shows a sample time series over Lake Victoria within the Upper Nile derived from the ExtR filter compared to the Hydroweb and DAHITI time series. It can be seen from the figure that the ExtR time series are close to the retracked time series of DAHITI (i.e., 0.94 average correlation) and to a lesser degree to Hydroweb (i.e., 0.92 average correlation). Overall, the correlations from both Hydroweb and DAHITI are high (i.e., > 0.90) and are statistically significant at 95% confidence level thus indicating a good performance of ExtR. More virtual stations are provided by Hydroweb along the Nile River (see Figure 1), which are used for comparison with the ExtR results. The average estimated RMSE and correlations are presented in Table 2. The ExtR results are 37.44 (on average at 95% confidence level) more correlated to Hydroweb data. Based on these in-situ validations, the ExtR algorithm is further justified and thus employed in this study to retrack satellite radar altimetry data.

3.2. Water storage changes

Assuming the contribution of ice/snow and vegetation to be negligible over the NRB, changes in TWS (ΔTWS) can be sufficiently taken to be the summation of changes in surface water (ΔSr), soil moisture (ΔSm), and groundwater (ΔGr) storages (e.g., Eq.1).

$$\Delta TWS = \Delta Sr + \Delta Sm + \Delta Gr. \tag{1}$$

GRACE products provide the total water storage changes ΔTWS while ΔSr are calculated from water level measurements as discussed in Section 3.2.1. The changes in soil moisture ΔSm

Table 2: A comparison between satellite altimetry values derived from the ExtR retracking method and those from in-situ water level measurements. The improvements in the RMSE are calculated using the in-situ measurements in comparison to the raw altimetry data.

	Raw altimetry data		**ExtR retracking**		
Stations	**RMSE** (cm)	**Correlation**	**RMSE** (cm)	**Correlation**	**Improvement (%)**
(1) Jinja	48.49	0.52	31.45	0.78	35.14
(2) Entebbe	61.14	0.66	36.04	0.95	41.05
(3) Old Aswan	36.77	0.54	22.44	0.88	38.97
(4) Esna	27.27	0.52	15.36	0.91	43.67
(5) Naga Hammadi	38.73	0.61	28.12	0.82	27.40
(6) Assiut	42.62	0.57	25.89	0.93	39.26
(7) Nubaria	25.87	0.62	16.19	0.92	37.44
(8) Hydroweb	56.13	0.59	29.28	0.94	47.83

Figure 2: A comparison between height time series of Lake Victoria obtained from the ExtR retracking method (black), DAHITI (red), and HYDROWEB (blue). The results of ExtR retracking method are highly correlated with those of HYDROWEB and DAHITI (i.e., $>$ 0.90; significant at 95% confidence level). This justifies the usage of the ExtR retracking method to obtain the surface heights of the 62 virtual stations along the NRB

are estimated from multi-models' outputs as discussed in Section 3.2.2. Using these estimates of ΔSr and ΔSm in Eq.1, the estimates of groundwater ΔGr within the NRB are derived.

3.2.1. Surface water storage changes

To calculate changes in surface water storage from water level data, the approach proposed in Frappart et al. (2008) is used. The process begins by generating water level maps at monthly scales using altimetry-derived in-situ and Hydroweb time series across the NRB. These maps are constructed at 1°×1° (similar to those of GRACE TWS) using point-wise water level time series and a bilinear interpolation scheme to estimate water levels at each grid point. Afterwards, the surface water volume changes (ΔSr) between two consecutive months i and $i-1$ within the basin S, corresponding to the difference of surface water level maps, is estimated by (see, e.g., Frappart et al., 2008, 2011),

$$\Delta Sr(i, i-1) = R_e^2 \delta\lambda\delta\theta \sum_{j \in S} P_j \delta h_j(\lambda, \theta, i, i-1) sin(\theta_j), \tag{2}$$

where $\delta\lambda$ and $\delta\theta$ are the sampling grid steps in longitude (λ) and latitude (θ) directions, respectively. R_e is the radius of the Earth ($\sim 6378\,km$), δh represents the difference of surface water levels, and $R_e^2 sin(\theta_j)\delta\lambda\delta\theta$ corresponds to the elementary surface of areas j. The percentage of inundation P_j is acquired from Multisatellite Inundation Data Set approach (Prigent et al., 2001, 2007).

3.2.2. Soil moisture changes

In order to achieve more reliable estimates of soil moisture changes over the NRB, data from three different sources (FLDAS-NOAH, WGHM, and ERA-Interim) are merged using the Triple Collocation Analysis (TCA; Gruber et al. (2017)) following (Stoffelen, 1998)). TCA is chosen since in the absence of ground reference data, it is the most popular method for estimating random error variances (Gruber et al., 2017)). TCA is applied here to merge soil moisture outputs;

$$S_1 = \alpha_1 S_t + e_1, \tag{3}$$

$$S_2 = \alpha_2 S_t + e_2, \tag{4}$$

$$S_3 = \alpha_3 S_t + e_3, \tag{5}$$

with S_t being the true soil moisture variation, S_1, S_2, and S_3 represents three soil moisture anomalies related to S_t with α_1, α_2, and α_3 being the coefficients that correspond to the errors

of e_1, e_2, and e_3, respectively. The objective is to estimate error variances associated with e_1, e_2, and e_3 to be used in the weighting process. On the one hand, TCA solves this by considering the errors of the products to be independent of each other while on the other hand, it arbitrarily assumes any of the products as a reference (see Stoffelen, 1998; Yilmaz et al., 2012, for more details regarding TCA implementation). By selecting any of the products as the reference, no impact is imposed on the merged time series (Gruber et al., 2017). Once the error variances are calculated, they are used in Eq. 6–8 to estimate weights of each merged product through

$$w_1 = \frac{\sigma {S_2}^2 \sigma {S_3}^2}{\sigma {S_1}^2 \sigma {S_2}^2 + \sigma {S_1}^2 \sigma {S_3}^2 + \sigma {S_2}^2 \sigma {S_3}^2}, \tag{6}$$

$$w_2 = \frac{\sigma {S_1}^2 \sigma {S_3}^2}{\sigma {S_1}^2 \sigma {S_2}^2 + \sigma {S_1}^2 \sigma {S_3}^2 + \sigma {S_2}^2 \sigma {S_3}^2}, \tag{7}$$

$$w_3 = \frac{\sigma {S_1}^2 \sigma {S_2}^2}{\sigma {S_1}^2 \sigma {S_2}^2 + \sigma {S_1}^2 \sigma {S_3}^2 + \sigma {S_2}^2 \sigma {S_3}^2}, \tag{8}$$

where $\sigma {S_1}^2$, $\sigma {S_2}^2$, and $\sigma {S_3}^2$ are error variances of S_1, S_2, and S_3, respectively, with the corresponding weights of w_1, w_2, and w_3. The final merged soil moisture estimate (Sm) is obtained by,

$$Sm = w_1 S_1 + w_2 S_2 + w_3 S_3. \tag{9}$$

A schematic illustration of the applied processing steps in this study, i.e., data integration procedure, retracking, and water storage estimations, is provided in Fig. 3.

4. Results and discussion

4.1. River height variations

First, a review of the altimetry-derived river level height time series (Fig. 4) is undertaken to understand the river's fluctuations with time. Thus, water lever time series is calculated for each virtual station within the three study regions of Fig. 1. The average of the stations' level height variations in each region is presented in Fig. 4. Also, the trend for different parts of time series are plotted (cf. black solid lines in Fig. 4). As can be seen from Figure 4, despite some similar behaviours such as positive trends after 2007 for all regions, the river height fluctuations differ from region to region. Between 1992-2002, water levels rose in the Upper and Central Nile regions, while in contrast, over the same period of time, water level fell at a rate of 0.01 m/year in the Lower Nile region. Moreover, unlike the Upper and Central

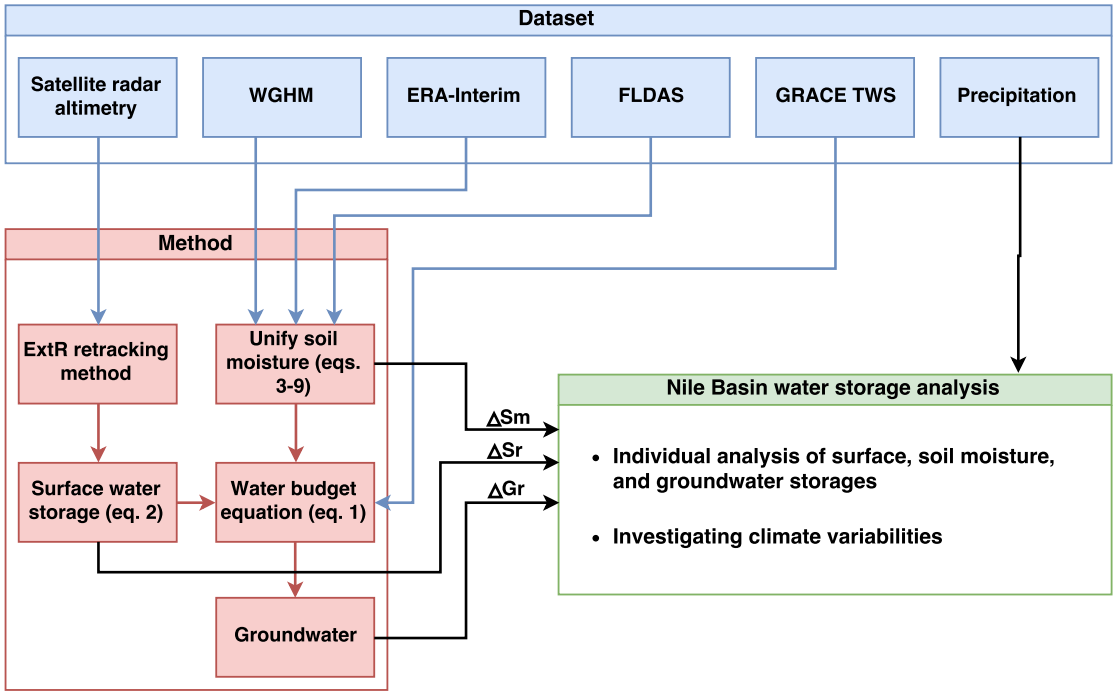

Figure 3: A schematic illustration of the applied methodology. The figure shows how the various stored water compartments; surface water, soil moisture and groundwater of the NRB are generated from multi-satellite and multi-models.

Nile regions, the Lower Nile region experienced water level fall in 2002. The Upper Nile region shows remarkably larger variations possibly due to higher rainfall in the region.

A decrease in the Upper Nile's water levels between 2002 and 2006 is consistent with the findings of Awange et al. (2008) and Swenson et al. (2009), where excessive dam construction (e.g., expansion of the Nalubaale Dam to include Kiira Dam) contributed to the fall. A similar negative trend is observed in the Lower Nile (0.76 average correlation between water levels of the Upper and Lower Nile) and Central Nile (0.68 average correlation). These correlations depicts the effects of Upper Nile's water management policies (e.g., dam constructions) on the other regions. The small change in the Central Nile during the period 2002-2006 compared to the Upper Nile could indicate other factors (e.g., climatical) since the Blue Nile comes from the Ethiopian highlands and as such was not impacted by the expansion of the dam in Uganda. This can explain the lower correlation between water level variations in Upper Nile and the Central Nile in comparison to the Lower Nile. The rate of fall in 2002-2006 in the lower Nile is higher than the upper and Central Nile as a result of the possible combined effects of anthropogenic

(Upper Nile; for example irrigation (see, e.g., Sultan et al., 2013; Awange et al., 2014b)) and climatic (Central Nile).

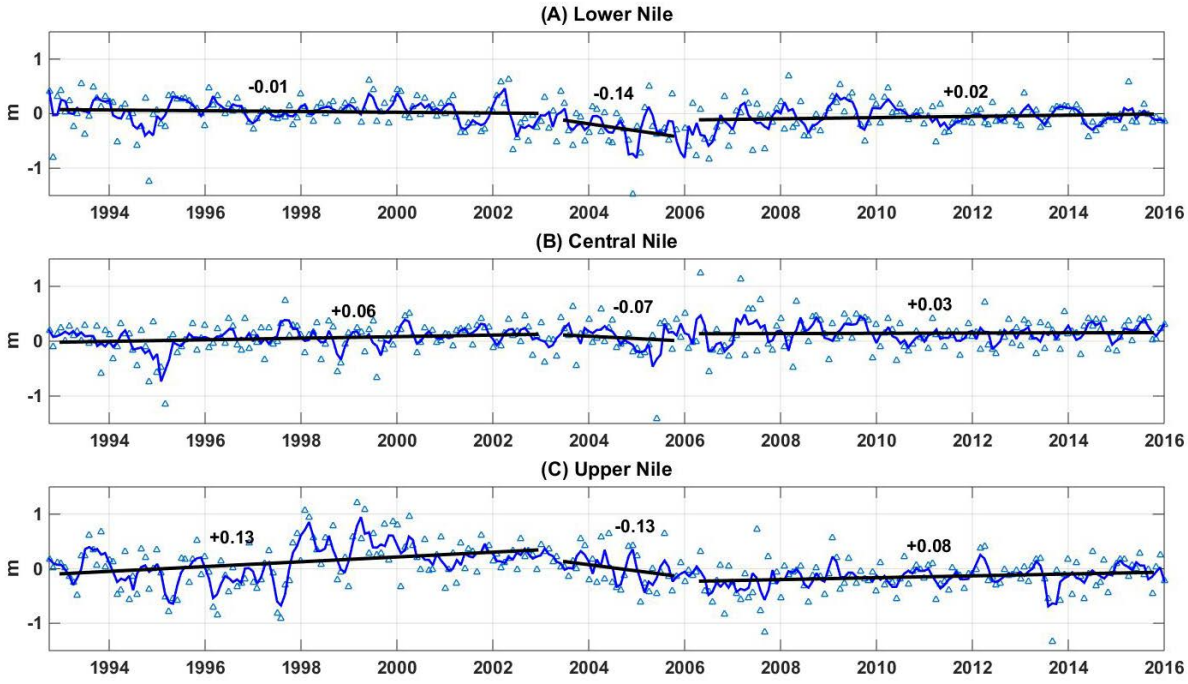

Figure 4: River level height variations (blue triangles) and their 60-day smoothed (for a better presentation) time series (blue lines) for each region. Variation rate (m/year) are reported above the fitted lines (black lines). Note that long-term average height levels are removed from each time series.

After 2006, water levels rose in all the three regions at different rates (i.e., 0.08 m/year for Upper Nile region, 0.03 m/year for Central Nile and 0.02 m/year for the Lower Nile region). These differences could be attributed to the ENSO rainfall of 2007 (Omondi et al., 2013), which brought heavy rainfall in the Upper Nile and La Niña, which caused drought in Ethiopia (which supplies the Blue Nile) leading to a smaller water level increase in the Central Nile over the same period of time. Furthermore, much of the White Nile's waters are lost in the Sudd-wetland (Awange et al., 2014a), hence, the diminishing effect of the increase can be seen from the Upper Nile to the Central Nile. The Lower Nile reflects water flow from the Central Nile although it is slightly lower (0.02 m/year), which can be explained possibly by withdrawal for irrigation purposes (see, e.g., Sultan et al., 2013; Awange et al., 2014b).

4.2. Water storages: surface, soil moisture and groundwater

Following Frappart et al. (2008), surface water storage is derived from water level fluctuations over the NRB. The average surface storage time series for the Upper, Central, and Lower Nile regions are shown in Fig. 5. The average time series of precipitation and GRACE TWS are also shown in the figure. It can be seen from the figure that the time series generally follow water level variation patterns of Fig. 4. The Upper Nile's time series depicts larger variations with various trends (see also the Lower Nile with a negative trend) unlike the Central Nile. Similar to the water level variation time series in Fig. 4, various smaller (short-term) trends can be found in be seen, particularly for the Upper and Lower Nile regions. The A negative trend in surface water seen before 2002 in the Lower Nile does not exist in the Upper or Central Nile regions possibly due to extensive usage in activities such as irrigations (see, e.g., Sultan et al., 2013).

Overall, the largest fluctuations are observed in the Upper Nile mainly due to high precipitation. TWS changes naturally follow the precipitation and hence a similar pattern can also be seen. This is followed by the Central Nile, which shows larger variations in both precipitation and TWS time series compared to the Lower Nile (a region with the least precipitation). Surface water changes in the Lower Nile, however, show larger variations possibly due to the stronger connection between this storage component over the entire basin.

As with water level variations (cf. Fig. 4), negative surface water storage trends exist in all the three regions (see Fig. 5) between 2002 and 2006 due to similar reasons discussed in Sect. 4.1. This, however, is followed by positive trends in all the regions. These trends are also evident in TWS variations over the Central and Upper Nile. Nevertheless, it can be seen that the TWS variation over the Lower Nile is generally negative, which can be attributed to the larger water usages in the region as discussed in Sect. 4.1. Low precipitation during this period can also be responsible for some part of this TWS negative changes. Also, the impacts of precipitation can be observed in several strong rise and fall in both surface water storage and TWS variations' time series. For example, strong precipitation in 2000 largely affected surface storage over the entire basin. The 2007 ENSO rainfall (Omondi et al., 2013) has the same impact on both surface water and TWS time series.

The results of TCA are presented in Fig. 6, which shows the average estimated soil moisture from FLDAS-NOAH, WGHM, and ERA-Interim over the Lower, Upper, and Central Nile

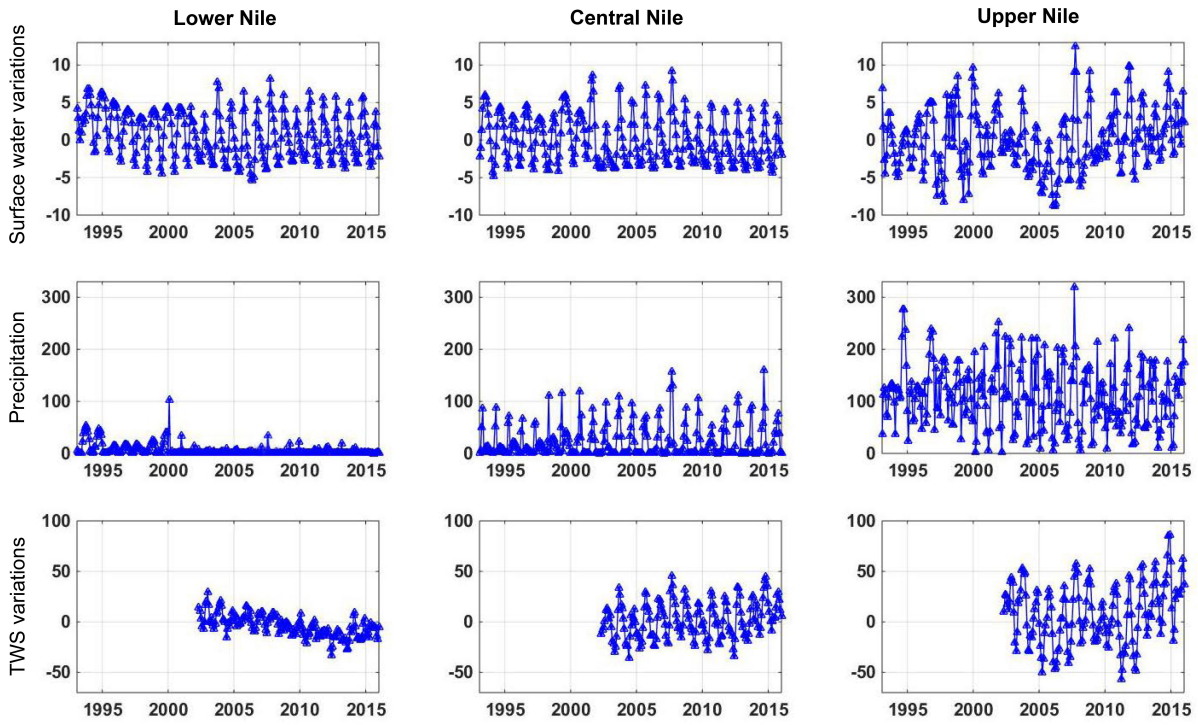

Figure 5: Average surface water storage, precipitation, and TWS variations over the Lower, Central, and Upper Nile regions. The temporal coverage of TWS is limited to 2002 to 2016 subject to the availability of GRACE data.

regions. Furthermore, using the surface water storage, soil moisture, and TWS changes, groundwater changes calculated based on Eq. 1 are also presented in Fig. 6. Following the patterns of precipitation and TWS time series in Fig. 5, smaller soil moisture and groundwater variations exist over the Lower Nile and to a lesser degree over the Central Nile compared to the Upper Nile while no considerable trend is observed in soil moisture variations. Groundwater changes exhibit short-term and long-term trends over different regions. Negative trends can be seen between 2002 and 2006 generally over the Upper and Central Nile, followed by remarkable increases, likely due to the same reasons explained earlier, see also (Awange et al., 2008). More importantly, a negative groundwater trend is dominant over the Lower Nile. This trend exists over the entire study period regardless of precipitation trends, which shows considerable groundwater depletion over the region. The rate of this decline, however, is found to be larger after 2008. As explained, reducing water controls in the Upper Nile after 2006 and the impact of the 2007 ENSO likely caused groundwater increase over the Central and Upper Nile and smaller negative trend over the Lower Nile. Nevertheless, this effect is found to be degraded

by 2008 resulting in negative trends (with a higher rate for the Lower Nile) in all groundwater time series between 2008 and 2012. Increasing amount of precipitation after 2012 caused groundwater to rise in both Upper and Central Niles. This high rainfall has the same impact on soil moisture variation between 2012 and 2016.

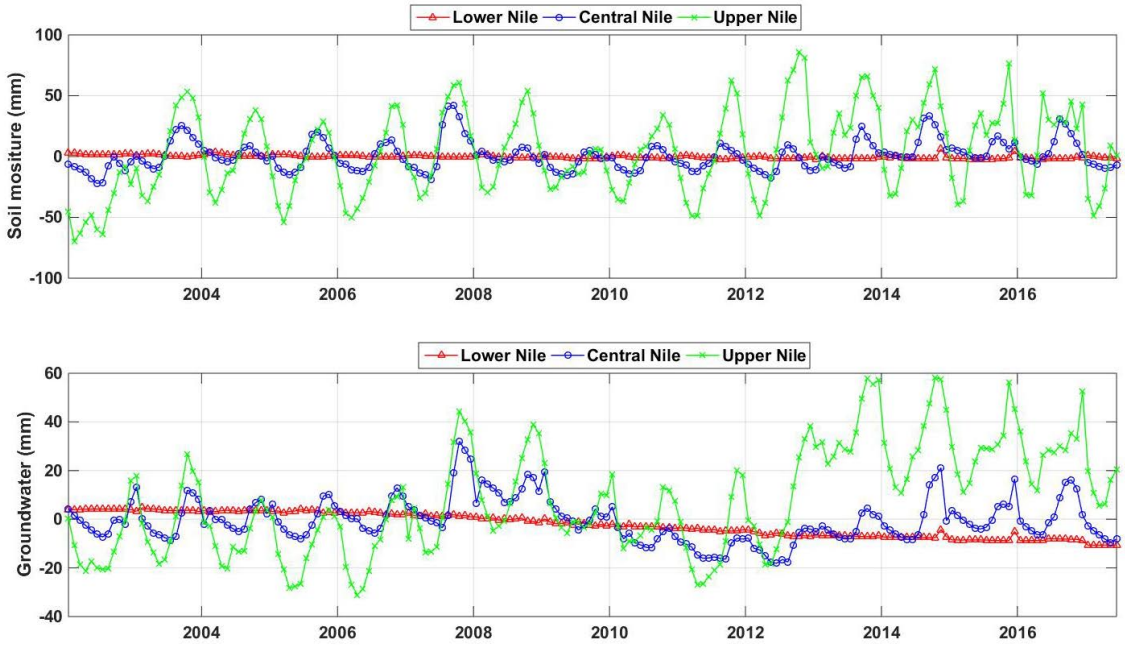

Figure 6: Average soil moisture and groundwater variations over the Lower, Central, and Upper Nile. Larger variations are clearly seen over the Upper Nile and to a lesser degree over the Central Nile. Contrary to the soil moisture time series, trends can be observed for groundwater time series, especially for the Lower Nile.

For each water storage compartment (surface water storage, groundwater, and soil moisture variations), the time series are averaged over each grid point for the period of 2002 to 2016 to generate the spatial pattern maps displayed in Fig. 7. It can clearly be seen that the Lower Nile depicts negative variations in the surface storage and groundwater. The Central Nile on the other hand does not show considerable change in most of the cases. Larger variations in terms of amplitude are found in the Upper Nile, thus confirming the previous findings. Besides negative groundwater changes in Egypt indicating huge usage (cf. Sultan et al., 2013; Awange et al., 2014b), Sudan and South Sudan also show considerable decline. In terms of surface water storage, the Upper Nile generally depicts positive variations.

To better compare the water storage changes within the various compartments, Fig. 8 show surface storage and groundwater trends neglecting those of soil moisture that indicated

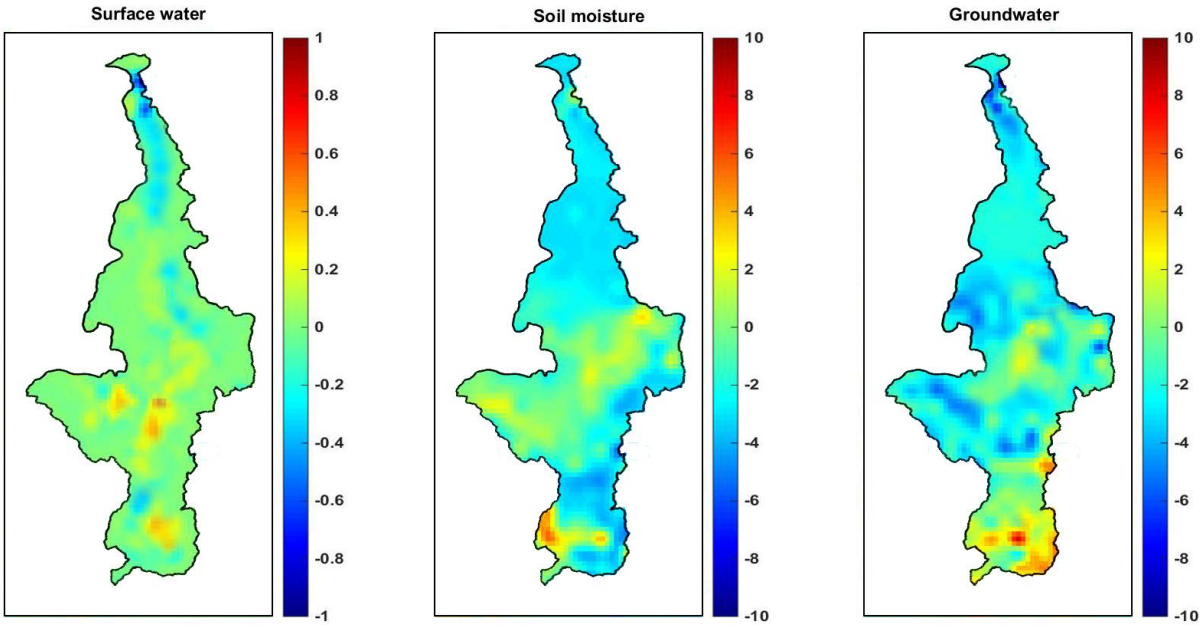

Figure 7: Temporally averaged surface water storage, soil moisture, and groundwater over the Nile Basin for the period 2002-2016.

no considerable change in Fig. 6. Negative trends are observed for both surface water and groundwater storages over the Lower Nile, with the latter being more prominent thus corroborating the conclusions of Sultan et al. (2013) and Awange et al. (2014b). No considerable surface storage trend is found for the Central Nile while the Upper Nile depicts positive values. Negative trends can also be seen in some parts of the Central Nile (e.g., in some parts of Sudan and Ethiopia) and in the Lower Nile (mostly in Egypt). In contrast, most parts of the Upper Nile shows positive groundwater trends.

4.3. Global teleconnections

In order to further understand the interactions of precipitation, river level heights, and TWS with climate variabilities, their correlations with ENSO climate variability index are calculated for each region and presented in Table 3. Those of IOD were low and statistically insignificant and as such are not shown. Table 3 show the highest correlation to be between ENSO and precipitation especially for the Upper Nile. For the correlations between ENSO and TWS, the highest value is also achieved in the Upper Nile probably due to the strong connection between precipitation and TWS over the region (see e.g., Awange et al., 2014a). For all variables

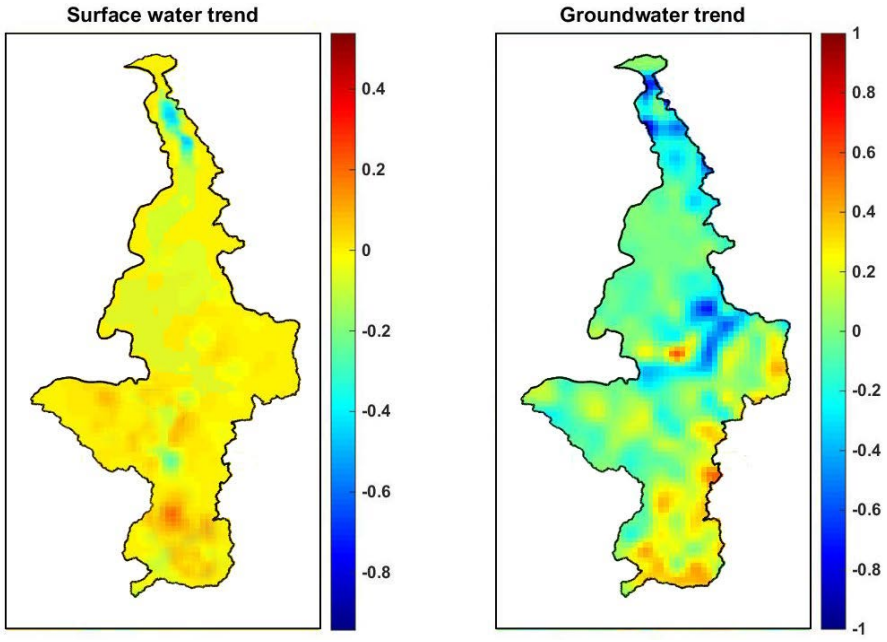

Figure 8: Surface water storage and groundwater trend over the Nile Basin for the period of 2002 to 2016. Trends of soil moisture that indicated no considerable change in Fig. 6 are neglected here.

Table 3: Correlations (at 0.05 significant level) between the river level heights, precipitation, and TWS time series for each region and climate variabilities of ENSO (those of IOD are not shown as they were small and insignificant). Note that cross-correlation is applied to account for lag differences between the time series.

Climate index	Variable	Lower Nile	Central Nile	Upper Nile
ENSO	Water level	0.47	0.52	0.58
	Precipitation	0.61	0.68	0.72
	TWS	0.58	0.64	0.69

(water level, precipitation, and TWS), the smallest correlations are achieved in the Lower Nile, a factor which can be attributed to very limited precipitation on the one hand, and high human impacts on water storages on the other hand (e.g., Sultan et al., 2013). Comparing ENSO's correlations between water levels and TWS, larger values are obtained with TWS. This can be explained by the fact that contrary to the water level fluctuations, non-climatic impacts on TWS are smaller. Considering the entire NRB, a higher correlation between the river level heights and climate indexes are found in the Central Nile (0.52 for ENSO). The addition of the Blue Nile in this area could possibly explain this higher correlation in comparison to the other regions.

5. Conclusion

This study analyzed the Nile River water level fluctuations and total water storage (TWS) compartments (surface water, soil moisture, and groundwater storage) using multi-mission satellite products, as well as land surface models. The association between these variables and climate variabilities are also investigated using precipitation and ENSO time series. This is crucial for water management policies of the Nile Basin Authority that manages the water resources on behalf of the eleven countries whose livelihood is highly dependent on the Nile for various aspects, e.g., water supply, agriculture, and industry. The following summarizes the outcomes of the study.

- A considerable long-term (2002-2016) negative groundwater trend is found in the Lower Nile (Egypt) signifying a potential depletion. The rate of decline is seen to increase rapidly from 2008 despite increase in precipitation and TWS time series, thus signifying the possibility of human usage, e.g., for irrigation purposes. Smaller soil moisture and groundwater variations exist over the Lower Nile and to a lesser degree over the Central Nile compared to the Upper Nile. While no considerable trend is observed for soil moisture variations, groundwater changes exhibit short-term and long-term trends over different regions. Negative trends are found between 2002 and 2006 over the Upper and Central Nile.

- The Upper Nile, the headwaters of the White Nile, depicts large water level variations compared to the Central (region covering the Blue Nile) and the Lower Nile (Egypt and Sudan). In general, a negative trend is found for water level variation in the Lower Nile (with the highest for the period 2002 – 2006) in contrast to the Central and Upper Nile.

- Larger correlation between the river level variations and precipitation exist in the Central Nile compared to the Upper and Lower Nile regions over the study period. The contribution of the Blue Nile (originating from the Ethiopian highlands) appears to cushion the Central Nile.

- Larger precipitation and TWS variations exist in the Upper Nile and to a lesser degree over the Central Nile, which can explain larger water storage fluctuation in these regions compared to the Lower Nile. Contrary to the Upper and Central Niles, negative trends are found for TWS variations over the Lower Nile.

- In addition to the trends, several strong impacts of precipitation, e.g., the 2007 ENSO rains, are also observed leading to strong rise and fall in both surface water storage and TWS variations time series.

- Large correlation between the precipitation and ENSO is found with an average of 0.67 indicating that precipitation and correspondingly surface water in the Nile Basin follows the global climate variability. ENSO had the most correlations with the three variables over the Central and Upper Nile in comparison to IOD.

Acknowledgement

M. Khaki is grateful for the research grant of Curtin International Postgraduate Research Scholarships (CIPRS)/ORD Scholarship provided by Curtin University (Australia). This work is a TIGeR publication.

References

Aboulela, H. (2012); Contribution of Satellite Altimetry Data in the Environmental Geophysical Investigation of the Northern Egyptian Continental Margin. International Journal of Geosciences, Vol. 3 No. 3, pp. 431-442, http://dx.doi.org/10.4236/ijg.2012.33047.

Agrawal, A.G., Petersen, L.R. (2003); Human immunoglobulin as a treatment for West Nile virus infection. J Infect Dis 188, 14, http://dx.doi.org/10.1086/376871.

Ahmed, A.A., El Daw, A.K. (2004); An Overview on Cooperation of Trans-Boundary water: Case of the Nile River Basin, the 2nd Regional Arab water conf, Cairo, Egypt.

Ahmed, A.A., Ismail, U.A.E. (2008); Sediment in the Nile River System, Consultancy Study requested by UNESCO.

Ahmed, A.E., Roghim, S., Saleh, A. (2014); Poverty Determinants in South Sudan: The Case of Renk County, Asian Journal of Agricultural Extension, Economics & Sociology 4(2): 125-136, 2015; Article no. AJAEES.2015.013, ISSN: 23207027, http://dx.doi.org/10.9734/AJAEES/2015/12724.

Ahmed, B.M., El Hussein, A.M., EL Khider, A.O. (2005); Some observations on ticks (Acari: Ixodidae) infesting sheep in River Nile Province of Northern Sudan. Onderstepoort Journal of Veterinary Research, 72:239243.

Alsdorf, D.E., Rodrguez, E., Lettenmaier, D.P. (2007); Measuring surface water from space, Rev. Geophys., 45, RG2002, http://dx.doi.org/10.1029/2006RG000197.

Awange, J.L., Sharifi, M.A., Ogonda, G. et al. (2008); The Falling Lake Victoria Water Level: GRACE, TRIMM and CHAMP Satellite Analysis of the Lake Basin. Water Resour Manage, 22: 775, http://dx.doi.org/10.1007/s11269-007-9191-y.

Awange, J.L., Forootan, E., Kusche, J., Kiema, J.B.K., Omondi, P.A.,Heck, B., Fleming, K., Ohanya, S.O., Gonalves, R.M. (2013a); Understanding the decline of water storage across the Ramser-Lake Naivasha using satellite-based methods, Advances in Water Resources, Volume 60, October 2013, Pages 7-23, ISSN 0309-1708, http://dx.doi.org/10.1016/j.advwatres.2013.07.002.

Awange, J.L., Anyah, R., Agola, N., Forootan, E., Omondi, P. (2013b); Potential impacts of climate and environmental change on the stored water of Lake Victoria Basin and economic implications, Water Resour. Res., 49, 81608173, http://dx.doi.org/10.1002/2013WR014350.

Awange, J.L., Gebremichael, M., Forootan, E., Wakbulcho, G., Anyah, R., Ferreira, V.G., Alemayehu, T. (2014a); Characterization of Ethiopian mega hydrogeological regimes using GRACE, TRMM and GLDAS datasets, Advances in Water Resources, Volume 74, December 2014, Pages 64-78, ISSN 0309-1708, http://dx.doi.org/10.1016/j.advwatres.2014.07.012.

Awange, J.L., Forootan, E., Kuhn, M., Kusche, J., Heck, B. (2014b); Water storage changes and climate variability within the Nile Basin between 2002 and 2011. Advances in Water Resources, 73:115, http://dx.doi.org/10.1016/j.advwatres.2014.06.010.

Awange, J.L., Ferreira, V.G., Forootan, E., Khandu, Andam-Akorful, S.A., Agutu, N.O. and He, X.F. (2016); Uncertainties in remotely sensed precipitation data over Africa. Int. J. Climatol., 36: 303323, http://dx.doi.org/10.1002/joc.4346.

Awulachew, S.B., Demissie, S.S., Hagos, F., Erkossa, T., Peden, D. (2012); Water management intervention analysis in the Nile Basin. In S. B. Awulachew, V. Smakhtin, D. Molden, &

493 D. Peden (Eds.), The Nile River Basin: Water, agriculture, governance and livelihoods (pp.
494 292311). Oxon,UK: Routledge.

495 Ayana, E.K., Awulachew, Bekele, S. (2008); Comparison of irrigation performance based
496 on management and cropping types. In Awulachew, Seleshi Bekele; Loulseged, Makon-
497 nen; Yilma, Aster Denekew (Comps.). Impact of irrigation on poverty and environment in
498 Ethiopia: draft proceedings of the symposium and exhibition, Addis Ababa, Ethiopia, 27-29
499 November 2007. Colombo, Sri Lanka: International Water Management Institute (IWMI).
500 pp.14-26.

501 Barnston, A.G., Livezey, R.E. (1987); Classification, seasonality, and persistence of low-
502 frequency atmospheric circulation patterns. Mon. Weather Rev. 115: 10831126.

503 Becker, M., Lovel, W., Cazenave, A., Gntner, A., Crtaux, J.F. (2010); Re-
504 cent Hydrological Behavior of the East African Great Lakes Region Inferred from
505 GRACE, Satellite Altimetry and Rainfall Observations. Comptes Rendus Geoscience,
506 http://dx.doi.org/10.1016/j.crte.2009.12.010.

507 Benada, J.R. (1997); PODAAC Merged GDR (TOPEX/POSEIDON) Generation B User's
508 Handbook, Version 2.0. JPL D-11007. Pasadena: Jet Propulsion Laboratory, California In-
509 stitute of Technology.

510 Berry, P.A.M., Garlick, J.D., Freeman, J.A., Mathers, E.L. (2005); Global Inland Wa-
511 ter Monitoring from Multi-Mission Altimetery. Geophysical Research Letter 32: L16401,
512 http://dx.doi.org/10.1029/2005GL022814.

513 Beyene, T., Lettenmaier, D.P., Kabat, P. (2010); Hydrologic impacts of climate change on the
514 Nile River Basin: implications of the 2007 IPCC scenarios. Climatic Change, Volume 100,
515 Issue 34, pp 433461, https://doi.org/10.1007/s10584-009-9693-0

516 Birkett, C.M. (1995); The Contribution of TOPEX/POSEIDON to the Global Monitoring of
517 Climatically Sensitive Lakes. Journal of Geophysical Research 25: 17925.

518 Birkett, C., Murtugudde, R., Allan, T. (1999); Indian Ocean climate event brings floods to
519 East Africa's lakes and the Sudd Marsh. GRL, 26(8), pp.1031-1034.

520 Birkett, C.M., Mertes, L.A.K., Dunne, T., Costa, M.H., Jasinski, M.J. (2002); Surface Wa-
521 ter Dynamics in the Amazon Basin: Application of Satellite Radar Altimetry. Journal of
522 Geophysical Research 107, http://dx.doi.org/10.1029/2001JD000609.

523 Boergens, E., Dettmering, D., Schwatke, C., Seitz, F. (2016); Treating the Hooking Effect in
524 Satellite Altimetry Data: A Case Study along the Mekong River and Its Tributaries. Remote
525 Sens., 8, 91, http://dx.doi.org/10.3390/rs8020091.

526 Brown, G.S. (1977); The Average Impulse Response of a Rough Surface and Its Applications.
527 IEEE Transactions on Antennas and Propagation 25: 6774.

528 Calmant, S., Seyler, F., Cretaux, J.F. (2008); Monitoring Continental Surface Waters by Satel-
529 lite Altimetry. Surveys in Geophysics 29, http://dx.doi.org/10.1007/s10712-008-9051-1.

530 Camberlin, P. (2009); Nile Basin Climates. Dumont, Henri J. The Nile: Origin, Environments,
531 Limnology and Human Use, Springer, pp.307-333, Monographiae Biologicae.

532 Cretaux , J-F., Jelinski, W., Calmant, S.Kouraev, A., Vuglinski, V., Berg Nguyen, M., Gennero,
533 M-C., Nino, F., Abarca Del Rio, R., Cazenave, A., Maisongrande, P. (2011); SOLS: A Lake
534 database to monitor in Near Real Time water level and storage variations from remote sensing
535 data, J. Adv. Space Res., http://dx.doi.org/10.1016/j.asr.2011.01.004.

536 Center for International Earth Science Information Network - CIESIN - Columbia University,
537 and Centro Internacional de Agricultura Tropical - CIAT. (2005); Gridded Population of the
538 World, Version 3 (GPWv3): Population Density Grid. Palisades, NY: NASA Socioeconomic
539 Data and Applications Center (SEDAC), http://dx.doi.org/10.7927/H4XK8CG2.

540 Center for International Earth Science Information Network - CIESIN - Columbia University.
541 (2016); Gridded Population of the World, Version 4 (GPWv4): Population Density Adjusted
542 to Match 2015 Revision UN WPP Country Totals. Palisades, NY: NASA Socioeconomic Data
543 and Applications Center (SEDAC), http://dx.doi.org/10.7927/H4HX19NJ.

544 Center for International Earth Science Information Network - CIESIN Columbia Uni-
545 versity. (2016); Documentation for the Gridded Population of the World, Version 4
546 (GPWv4). Palisades NY: NASA Socioeconomic Data and Applications Center (SEDAC).
547 http://dx.doi.org/10.7927/H4D50JX4.

548 Chen, J., Jegen-Kulcsar, M. (2007); The empirical mode decomposition (EMD) method in MT
549 data processing. - In: Ritter, O., Brasse, H. (Eds.), - Protokoll zum 22. Kolloquium Elek-
550 tromagnetische Tiefenforschung, 22. Kolloquium Elektromagnetische Tiefenforschung (Hotel
551 Maxiky, Dn, Czech Republic 2007), pp. 6776.

552 Cheng, M.K., Tapley, B.D. (2004); Variations in the Earth's oblateness during
553 the past 28 years. Journal of Geophysical Research, Solid Earth, 109, B09402.
554 http://dx.doi.org/10.1029/2004JB003028.

555 Coe, M.T., Birkett, C.M. (2004); Calculation of river discharge and prediction of lake height
556 from satellite radar altimetry: Example for the Lake Chad basin. Water Resour. Res., 40,
557 W10205, http://dx.doi.org/10.1029/2003WR002543.

558 Conway, D. (2002); Extreme Rainfall Events and Lake Level Changes in East Africa: Recent
559 Events and Historical Precedents. In E.O. Odada and D. O. Olago (eds.) The East African
560 Great Lakes: Limnology, Palaeolimnology and Biodiversity. Advances in Global Change Re-
561 search V. 12. Kluwer, Dordrecht. Pp. 63-92.

562 Conway, D. (2017); Water resources: future Nile river flows. Nature Climate Change, 7 (5). pp.
563 319-320. ISSN 1758-678X.

564 Davis, C.H. (1995); Growth of the Greenland Ice Sheet: A Performance Assessment of Altimeter
565 Retracking Algorithms. IEEE Transactions on Geo-Science and Remote Sensing 33 (5): 1108-
566 1116, http://dx.doi.org/10.1109/36.469474.

567 Davis, C. H. (1997); A Robust Threshold Retracking Algorithm for Measuring Ice-Sheet Surface
568 Elevation Change from Satellite Radar Altimeters. IEEE Transactions on Geoscience and
569 Remote Sensing 35 (4), http://dx.doi.org/10.1109/36.602540.

570 Dee, D. P., Uppala, S. M., Simmons, A. J., Berrisford, P., Poli, P., Kobayashi, S., Andrae, U.,
571 Balmaseda, M. A., Balsamo, G., Bauer, P., Bechtold, P., Beljaars, A. C. M., van de Berg, L.,
572 Bidlot, J., Bormann, N., Delsol, C., Dragani, R., Fuentes, M., Geer, A. J., Haimberger, L.,
573 Healy, S. B., Hersbach, H., Hlm, E. V., Isaksen, L., Kllberg, P., Khler, M., Matricardi, M.,
574 McNally, A. P., Monge-Sanz, B. M., Morcrette, J.-J., Park, B.-K., Peubey, C., de Rosnay, P.,
575 Tavolato, C., Thpaut, J.-N. and Vitart, F. (2011); The ERA-Interim reanalysis: configuration

576 and performance of the data assimilation system. Q.J.R. Meteorol. Soc., 137: 553597, doi:
577 10.1002/qj.828.

578 Döll, P., Kaspar, F., Lehner, B. (2003); A global hydrological model for deriving water avail-
579 ability indicators: model tuning and validation, J Hydrol 207:105134.

580 Döll, P., Mller Schmied, H., Schuh, C., Portmann, F.T., Eicker, A. (2014); Global-scale assess-
581 ment of groundwater depletion and related groundwater abstractions: Combining hydrologi-
582 cal modeling with information from well observations and GRACE satellites, Water Resour.
583 Res., 50, http://dx.doi.org/10.1002/2014WR015595.

584 Elshamy, M.E., Seierstad, I.A., Sorteberg, A. (2009); Impacts of climate change on Blue
585 Nile flows using bias-corrected GCM scenarios, Hydrol. Earth Syst. Sci., 13, 551-565,
586 http://dx.doi.org/10.5194/hess-13-551-2009.

587 FAO Land and Water Division. (1997); Irrigation potential in Africa; A basin approach. Food
588 and Agriculture Organization of the United Nations, Rome (Italy).

589 Flandrin, P., Gonalvs, P., Rilling, G. (2004); Detrending and denoising with empirical mode
590 decompositions, 12th European Signal Processing Conference, Vienna, 2004, pp. 1581-1584.

591 Forootan, E., Rietbroek, R., Kusche, J., Sharifi, M. A., Awange, J., Schmidt, M., Omondi,
592 P., Famiglietti, J. (2014); Separation of large scale water storage patterns over Iran using
593 GRACE, altimetry and hydrological data. Journal of Remote Sensing of Environment, 140,
594 580-595, http://doi.org/10.1016/j.rse.2013.09.025.

595 Forootan, E., Khandu, Awange, J., Schumacher, M., Anyah, R., van Dijk, A., Kusche, J.,
596 (2016); Quantifying the impacts of ENSO and IOD on rain gauge and remotely sensed
597 precipitation products over Australia. Remote Sensing of Environment,172, Pages 50-66,
598 http://dx.doi.org/10.1016/j.rse.2015.10.027.

599 Frappart, F., Calmant, S., Cauhope, M., Seyler, F., Cazenave, A. (2006); Preliminary results
600 of envisat ra-2-derived water levels validation over the amazon basin, Remote Sensing of
601 Environment, 100(2), 252-264.

602 Frappart, F., Papa, F., Famiglietti, J.S., Prigent, C., Rossow, W.B., Seyler, F. (2008); In-
603 terannual variations of river water storage from a multiple satellite approach: A case

study for the Rio Negro River basin. Journal of Geophysical Research, 113, D21104. doi:10.1029/2007JD009438.

Frappart, F. Papa, F., Gntner, A., Werth, S., da Silva, J.S., Tomasella, J., Seyler, F., Prigent, C., Rossow, W.B., Calmant, S., Bonnet, M.P. (2011); Satellite-based estimates of groundwater storage variations in large drainage basins with extensive floodplains, Remote Sensing of Environment, Volume 115, Issue 6, Pages 1588-1594, ISSN 0034-4257, https://doi.org/10.1016/j.rse.2011.02.003.

Fu, L.L., Christensen, E., Yamarone, C.A. (1994); TOPEX/POSEIDON mission overview. J. geophys. Res., 99, http://dx.doi.org/10.1029/94JC01761.

Goita, K., Diepkile, A.T. (2012); Radar altimetry of water level variability in the Inner Delta of Niger River. IEEE, International Geoscience and Remote Sensing Symposium (IGARSS), Munich, Germany, 5262-5265, http://dx.doi.org/10.1109/IGARSS.2012.6352422.

Gomez-Enri, J., Vignudelli, S., Quartly, G., Gommenginger, C., Benveniste, J. (2009); Bringing Satellite Radar Altimetry Closer to Shore. Remote Sensing, SPIE Newsroom, http://dx.doi.org/10.1117/2.1200908.1797.

Gruber, A., Dorigo, W.A., Crow, W., Wagner, W. (2017); Triple Collocation-Based Merging of Satellite Soil Moisture Retrievals, in IEEE Transactions on Geoscience and Remote Sensing, vol. 55, no. 12, pp. 6780-6792, doi: 10.1109/TGRS.2017.2734070.

Hassan, A.A., Jin, S. (2014); Lake level change and total water discharge in East Africa Rift Valley from satellite-based observations, In Global and Planetary Change, Volume 117, Pages 79-90, ISSN 0921-8181, https://doi.org/10.1016/j.gloplacha.2014.03.005.

Huang, N.E., Shen, Z., Long, S.R., Wu, M.C., Shih, H.H., et al. (1998); The empirical mode decomposition and the Hilbert spectrum for nonlinear and non-stationary time series analysis. Proceedings of the Royal Society of London A 454: 903-995.

Hwang, C.W., Kao, Y.H. (2010); A Preliminary Analysis of Lake Level and Water Storage Changes over Lakes Baikal and Balkhash from Satellite Altimetry and Gravimetry. Terrestrial, Atmospheric and Oceanic Sciences 22: 97108, http://dx.doi.org/10.3319/TAO.2010.05.19.01(TibXS).

Ismail, S.S., Samuel, M.G. (2011); Response of river Nile dredging on water levels. Fifteenth International Water Technology Conference, IWTC-15 2011, Alexandria, Egypt .

Khaki, M., Forootan, E., Sharifi, M.A. (2014); Satellite radar altimetry waveform retracking over the Caspian Sea. Int. J. Remote Sens., 35(17), 63296356, http://dx.doi.org/10.1080/01431161.2014.951741.

Khaki, M., Forootan, E., Sharifi, M.A., Awange, J., Kuhn, M. (2015); Improved gravity anomaly fields from retracked multimission satellite radar altimetry observations over the Persian Gulf and the Caspian Sea. Geophys. J. Int. 202 (3): 1522-1534, http://dx.doi.org/10.1093/gji/ggv240.

Khaki, M., Forootan, E., Kuhn, M., Awange, J., Longuevergne, L., Wada, W., (2018). Efficient Basin Scale Filtering of GRACE Satellite Products, In Remote Sensing of Environment, Volume 204, Pages 76-93, ISSN 0034-4257, https://doi.org/10.1016/j.rse.2017.10.040.

Khandu, Forootan, E., Schumacher, M., Awange, J.L., Mller Schmied, H. (2016); Exploring the influence of precipitation extremes and human water use on total water storage (TWS) changes in the Ganges-Brahmaputra-Meghna River Basin, Water Resour. Res., 52, 22402258, http://dx.doi.org/10.1002/2015WR018113.

Kizza, M., Rodhe, A., Xu, C.Y., Natle, K.H., Halldian, S., (2009); Temporal rainfall variability in the Lake Victoria Basin in east Africa during the twentieth century Theor. Appl. Climatol., 98, pp. 119-135.

Lee, H., Shum, C.K., Yi, Y., Ibaraki, M., Kim, J.W., Braun, A., Kuo, C.Y., Lu, Z. (2009); Louisiana Wetland Water Level Monitoring Using Retracked TOPEX/POSEIDON Altimetry. Marine Geodesy 32: 284302, http://dx.doi.org/10.1080/01490410903094767.

Lorenz, E. (1956); Empirical orthogonal function and statistical weather prediction. Technical Report Science Report No 1, Statistical Forecasting Project. MIT, Cambridge.

Martin, T.V., Zwally, H., Brenner, A.C., Bindschadler, R.A. (1983); Analysis and Retracking of Continental Ice Sheet Radar Altimeter Waveforms. Journal of Geophysical Research 88 (C3): 1608, http://dx.doi.org/10.1029/JC088iC03p01608.

659 Mayer-Gürr, T., Zehentner, N., Klinger, B., Kvas, A. (2014); ITSG-Grace2014: a new GRACE
660 gravity field release computed in Graz. - in: GRACE Science Team Meeting (GSTM), Pots-
661 dam am: 29.09.2014.

662 McNally, A., Arsenault, K., Kumar, S., Shukla, S., Peterson, P., Wang, S., Funk, C.,
663 Peters-Lidard, C.D., Verdin, J.P. (2017); A land data assimilation system for sub-Saharan
664 Africa food and water security applications. Scientific Data 4, Article number: 170012,
665 http://dx.doi.org/10.1038/sdata.2017.12.

666 Mohamed, Y.A., van den Hurk, B.J.J.M., Savenije, H.H.G., Bastiaanssen, W.G.M. (2005);
667 Impact of the Sudd wetland on the Nile hydroclimatology, Water Resour. Res., 41, W08420,
668 http://dx.doi.org/10.1029/2004WR003792.

669 Muala, E., Mohamed, Y.A., Duan, Z., van der Zaag, P. (2014); Estimation of Reservoir Dis-
670 charges from Lake Nasser and Roseires Reservoir in the Nile Basin Using Satellite Altimetry
671 and Imagery Data. Remote Sens., 6, 7522-7545.

672 Multsch, S., Elshamy, M.E., Batarseh, S., Seid, A.H., Frede, H.-G., Breuer, L. (2017); Im-
673 proving irrigation efficiency will be insufficient to meet future water demand in the Nile
674 Basin, Journal of Hydrology: Regional Studies, Volume 12, Pages 315-330, ISSN 2214-5818,
675 https://doi.org/10.1016/j.ejrh.2017.04.007.

676 Nazemosadat, M.J., Cordery, I. (2000); On the relationships between ENSO and autumn rainfall
677 in Iran. Int J Climatol 20:4761.

678 Nunzio, J. (2013); Conflict on the Nile: the future of transboundary water disputes over the
679 world's longest river. Dalkeith: Future Directions International.

680 Nurutami, M.N., Hidayat, R. (2016); Influences of IOD and ENSO to Indonesian
681 Rainfall Variability: Role of Atmosphere-ocean Interaction in the Indo-pacific Sector,
682 Procedia Environmental Sciences, Volume 33, 2016, Pages 196-203, ISSN 1878-0296,
683 http://dx.doi.org/10.1016/j.proenv.2016.03.070.

684 Omondi, P., Awange, J.L., Ogallo, L.A., Okoola, R.A., Forootan, E. (2012); Decadal rainfall
685 variability modes in observed rainfall records over East Africa and their relations to historical
686 sea surface temperature changes. Journal of Hydrology. 464-465: pp. 140-156.

687 Omondi, P., Awange, J.L., Ogallo, L.A., Ininda, J., Forootan, E. (2013); The influence of low
688 frequency sea surface temperature modes on delineated decadal rainfall zones in Eastern
689 Africa region. Advances in Water Resources. 54: pp. 161-180.

690 Papa, F., Durand, F., Rossow, W.B., Rahman, A., Bala, S. (2010); Satellite altimeter-derived
691 monthly discharge of the Ganga-Brahmaputra River and its seasonal to interannual variations
692 from 1993 to 2008. J. Geophys. Res., 115, C12013, http://dx.doi.org/10.1029/2009JC006075.

693 Papa, F., Frappart, F., Malbeteau, Y., Shamsudduha, M., Vuruputur, V., Sekhar, M., Ramil-
694 lien, G., Prigent, C., Aires, F., Pandey, R.K., Bala, S., Calmant, S. (2015); Satellite-derived
695 surface and sub-surface water storage in the GangesBrahmaputra River Basin, Journal of Hy-
696 drology: Regional Studies, Volume 4, Part A, September 2015, Pages 15-35, ISSN 2214-5818,
697 http://dx.doi.org/10.1016/j.ejrh.2015.03.004.

698 Prigent, C., Matthews, E., Aires, F., Rossow, W.B. (2001); Remote sensing of global wet-
699 land dynamics with multiple satellite data sets, Geophys. Res. Lett., 28, 4631 4634,
700 doi:10.1029/2001GL013263.

701 Prigent, C., Papa, F., Aires, F., Rossow, W.B., Matthews, E. (2007); Global inundation dynam-
702 ics inferred from multiple satellite observations, 1993 2000, J. Geophys. Res., 112, D12107,
703 doi:10.1029/2006JD007847.

704 Rao, S. A., Behara, S. K., Masumoto, Y., Yamagata, T. (2002); Interannual subsurface vari-
705 ability in the tropical Indian Ocean with a special emphasis on the Indian Ocean Dipole,
706 Deep Sea Res., Part II, 49, 1549 1572.

707 Reynolds, R.W., Smith, T.M., Liu, C., Chelton, D.B., Casey, K.S., Schlax, M.G. (2007); Daily
708 high-resolution blended analyses for sea surface temperature. J. Climate, 20, 5473-5496.

709 Rilling, G., Flandrin, P., Goncalves, P. (2003); On empirical mode decomposition and its algo-
710 rithms. in: Proceedings IEEE-EURASIP Workshop on Nonlinear Signal and Image Process-
711 ing NSIP-03, Grado I, p. 3.

712 Rogers, J. (1984); The Association between the North Atlantic Oscillation and the
713 Southern Oscillation in the Northern Hemisphere. Mon. Wea. Rev., 112, 19992015,
714 http://dx.doi.org/10.1175/1520-0493(1984)112¡1999:TABTNA¿2.0.CO;2.

715 Samuel, M.G. (2014); Limitations of navigation through Nubaria canal, Egypt. Journal of
716 Advanced Research, 5, 147155, http://dx.doi.org/10.1016/j.jare.2013.01.006.

717 Sandwell, D.T. (1990); Geophysical Applications of Satellite Altimetry. Reviews of Geophysics
718 Supplement, p. 132-137.

719 Schneider, U, Becker, A, Finger, P, Meyer-Christoffer, A, Rudolf, B, Ziese,
720 M. (2015); GPCC Full Data Reanalysis Version 7.0 at 1.0: Monthly Land-
721 Surface Precipitation from Rain-Gauges built on GTS-based and Historic Data,
722 http://dx.doi.org/10.5676/DWD_GPCC/FD_M_V7_100.

723 Schumacher M., Eicker, A., Kusche, J., Schmied, H.M., Dll, P. (2015); Covariance Analysis and
724 Sensitivity Studies for GRACE Assimilation into WGHM. In: Rizos C., Willis P. (eds) IAG
725 150 Years, International Association of Geodesy Symposia, vol 143. Springer, Cham.

726 Schwatke, C., Dettmering, D., Bosch, W., and Seitz, F. (2015); DAHITI an innovative approach
727 for estimating water level time series over inland waters using multi-mission satellite altimetry,
728 Hydrol. Earth Syst. Sci., 19, 4345-4364, http://dx.doi.org/10.5194/hess-19-4345-2015.

729 Seyler, F., Calmant, S., Santos da Silva, J., Filizola, N., Roux, E., Cochonneau, G., Vauchel,
730 P., Bonnet, M.-P. (2008); Monitoring water level in large trans-boundary ungauged basins
731 with altimetry: the example of ENVISAT over the Amazon basin. Journal of Applied Remote
732 Sensing, 7150: 715017, http://dx.doi.org/10.1117/12.813258.

733 Siam, M.S., Eltahir, E.A.B. (2015); Explaining and forecasting interannual vari-
734 ability in the flow of the Nile River, Hydrol. Earth Syst. Sci., 19, 1181-1192,
735 http://dx.doi.org/10.5194/hess-19-1181-2015.

736 Stoffelen, A. (1998); Toward the true near-surface wind speed: Error modeling and calibration
737 using triple collocation, J. Geophys. Res., 103(C4), 77557766.

738 Sultan, M., Ahmed, M., Sturchio, N., Eugene, Y., Milewski, A., Becker, R., Wahr, J., Becker,
739 D., Chouinard ,K. (2013); Assessment of the vulnerabilities of the Nubian sandstone fossil
740 aquifer, North Africa, in (R. A. Pielke, Editor), Climate Vulnerability: Understanding and
741 addressing threats to essential resources. Elsevier, 311-333 pp.

Swenson, S., Wahr, J. (2002); Methods for inferring regional surface-mass anomalies from Gravity Recovery and Climate Experiment (GRACE) measurements of time-variable gravity. Journal of Geophysical research, 107, B9, 2193. http://dx.doi.org/10.1029/2001JB000576.

Swenson, S., Wahr, J. (2006); Post-processing removal of correlated errors in GRACE data. Geophysical Research Letters, 33, L08402. http://dx.doi.org/10.1029/2005GL025285.

Swenson, S., Chambers, D., Wahr, J. (2008); Estimating geocentervariations from a combination of GRACE and ocean model output. Journal of Geophysical research, 113, B08410. http://dx.doi.org/10.1029/2007JB005338.

Swenson, S., Wahr, J. (2009); Monitoring the water balance of Lake Victoria, East Africa, from space, J. Hydrol., 370(14), 163176, http://dx.doi.org/10.1016/j.jhydrol.2009.03.008.

Taye, M.T., Ntegeka, V., Ogiramoi, N.P., Willems, P. (2011); Assessment of climate change impact on hydrological extremes in two source regions of the Nile River Basin, Hydrol. Earth Syst. Sci., 15, 209-222, http://dx.doi.org/10.5194/hess-15-209-2011.

Trenberth, K.E. (1990); Recent observed interdecadal climate changes in the Northern Hemisphere. Bull. Amer. Me- teor. Soc., 71,988-993.

Tropical Rainfall Measuring Mission (TRMM) (2011); TRMM (TMPA/3B43) Rainfall Estimate L3 1 month 0.25 degree x 0.25 degree V7, Greenbelt, MD, Goddard Earth Sciences Data and Information Services Center (GES DISC), Accessed [Data Access Date] https://disc.gsfc.nasa.gov/datacollection/TRMM_3B43_7.html.

Tseng, K.H., Shum, C.K. , Yi, Y., Fok, H.S., Kuo, C.Y., Lee, H., Cheng, X., Wang, X. (2013); Envisat Altimetry Radar Waveform Retracking of Quasi-Specular Echoes over the Ice-Covered Qinghai Lake. Terrestrial Atmospheric and Oceanic Science 24: 615627, http://dx.doi.org/10.3319/TAO.2012.12.03.01(TibXS).

Uebbing, B., Kusche, J., Forootan, E. (2015); Waveform retracking for improving level estimations from Topex/Poseidon, Jason-1 and -2 altimetry observations over African lakes, IEEE Trans. Geosci. Remote Sens., 53(4), 22112224.

Wahr, J.M., Molenaar, M., Bryan, F. (1998); Time variability of the Earth's gravity field: hydrological and oceanic effects and their possible detection using GRACE. J Geophys Res 108(B12):3020530229, http://dx.doi.org/10.1029/98JB02844.

771 Wingham, D.J., Rapley, C.G., Griffiths, H. (1986); New Techniques in Satellite Altimeter
772 Tracking Systems, ESA Proceedings of the 1986 International Geoscience and Remote Sensing
773 Symposium (IGARSS 86) on Remote Sensing. Todays Solutions for Tomorrows Information
774 Needs 3: 13391344.

775 Woodward, J.C., Macklin, M.G., Krom, M.D., Williams, M.A.J. (2007); The Nile: evolution,
776 Quaternary River Environments and material fluxes. In Large Rivers: Geomorphology and
777 Management. Wiley, Chichester, 261-292.

778 Worley, S.J., Woodruff, S.D., Reynolds, R.W., Lubker, S.J., Lott, N. (2005); ICOADS Re-
779 lease 2.1 data and products. Int. J. Climatol. (CLIMAR-II Special Issue), 25, 823-842,
780 http://dx.doi.org/10.1002/joc.1166.

781 Yang, L., Lin, M., Liu, Q., Pan, D. (2012); A Coastal Altimetry Retracking Strategy Based
782 on Waveform Classification and Sub-Waveform Extraction. International Journal of Remote
783 Sensing 33 (24): 78067819, http://dx.doi.org/10.1080/01431161.2012.701350.

784 Yilmaz, M.T.,Crow, W.T., Anderson, M.C., Hain, C.(2012); An objective methodology for
785 merging satellite and modelbased soil moisture products, Water Resour. Res., 48, W11502,
786 doi:10.1029/2011WR011682.

787 Yin, X., Nicholson, S.E. (1998); The water balance of Lake Victoria. Hydrol. Sci. J. Sci. Hydrol.
788 43 (5), 789811.

789 Zakharova, E., Kouraev, A., Cazenave, A. (2006); Amazon river discharge estimated from the
790 Topex/Poseidon altimetry, C. R. Geosci., 338, 188196.

791 Zaroug, M.A.H., Eltahir, E.A.B., Giorgi, F. (2014); Droughts and floods over the upper catch-
792 ment of the Blue Nile and their connections to the timing of El Nio and La Nia events,
793 Hydrol. Earth Syst. Sci., 18, 1239-1249, http://dx.doi.org/10.5194/hess-18-1239-2014.